SPATIAL PROFILES OF LINES IN ACTIVE REGION LOOPS

V. KRISHAN

Indian Institute of Astrophysics, Bangalore 560034, India

(Received 24 September, 1982; in final form 4 May, 1983)

Abstract. From the statistical treatment of magnetohydrodynamically turbulent plasma, a steady-state density, temperature and magnetic field structure is derived for a coronal loop emitting in UV and EUV range. Spatial variation of line flux is presented for the lines C II, C III, O IV, O VI, Ne VII, and Mg X. It is found that the hotter lines which are emitted near the surface of the loop have larger spatial extents compared to the lines originating in the cool core of the loop, in agreement with the observations.

1. Introduction

Solar active regions are found to be magnetically, spatially as well as temporally complex, the complexity being manifested through emissions at optical UV, EUV, and X-ray wavelengths (Foukal, 1975, 1976, 1978; Foukal *et al.*, 1974; Levine and Withbroe, 1977; Vaiana and Rosner, 1978). The most common geometrical form observed in the active regions looks like a loop or an arcade of loops essentially outlining the local magnetic field configuration. The loops are believed to contain current carrying plasma and therefore have a helical form of the magnetic field (Levine and Altschuler, 1974; Poletto *et al.*, 1975; Krieger *et al.*, 1976; Priest, 1978; Hood and Priest, 1979). High spatial resolution observations of lines of C II, C III, O IV, Ne VII, and Mg X indicate that in the steady state, a typical loop consists of a cool central core with temperature increasing towards the surface which merges with the hot corona outside (Foukal, 1976; Foukal *et al.*, 1974; Levine and Withbroe, 1977). In an earlier paper by Krishan (1982) a steady-state model of spot associated loops was presented where a steady-state configuration of the magnetoplasma including turbulence was derived purely from the statistical treatment of the magnetohydrodynamics of an incompressible fluid subjects to the invariance of total energy, magnetic helicity, and the magnetic flux. The treatment and the method used closely follows that of Montgomery *et al.* (1978). The steady state is describable by the superposition of Chadrasekhar–Kendall functions which are the eigenfunctions of the curl operator.

A single Chandrasekhar–Kendall function represents a force-free state but the superposition of these functions do not. Thus in general the steady state may have small departures from a force free state and it is possible to account for the discrepancies in the observed and the model force free state by the addition of more than one such states. The statistical mechanical treatment of magnetohydrodynamic turbulence as described by Montgomery *et al.* (1978) and applied to solar active regions by Krishan (1982) differs from the usual MHD stability theory in the sense that it does not involve small perturbation expansions and therefore is fully nonlinear. One of the main results of the statistical treatment is that even with initial quiescent conditions the system organises

Solar Physics **88** (1983) 155–161. 0038–0938/83/0881–0155$01.05.

itself in such a way that it has a finite root mean square turbulent velocity $\langle V^2 \rangle$. Using this theoretical model, magnetic field and temperature profiles of the loops were derived which fitted rather well with the observed cool core and hot sheath loop models. For the sake of completion and comprehension, we present here the magneto-hydrodynamical equations used to derive the temperature and magnetic field structure of a loop. In this paper, we calculate the line flux as a function of spatial coordinate transverse to the magnetic field. The relative spatial width of each line is estimated. It is found that the higher temperature lines (e.g. Ne VII, Mg X) which are excited towards the surface of the loop have, larger spatial widths than the cooler ones (e.g. C II, C III) excited in the core region. This is in line with the findings of Levine and Withbroe (1977).

2. Steady-State Model of Coronal Loops

We assume a cylindrical column of plasma with periodic boundary conditions at the ends of the cylinder. The magnetohydrodynamical equations for an incompressible medium are:

$$\rho\left[\frac{\partial \mathbf{V}}{\partial t} + (\mathbf{V}\cdot\nabla)\mathbf{V}\right] = \frac{1}{4\pi}(\nabla \times \mathbf{B}) \times \mathbf{B} - \nabla p + \rho \mathbf{g}\,, \tag{1}$$

$$\frac{\partial \mathbf{B}}{\partial t} = \nabla \times (\mathbf{V} \times \mathbf{B})\,, \tag{2}$$

$$\nabla \cdot \mathbf{B} = \nabla \cdot \mathbf{V} = 0\,, \tag{3}$$

where ρ is the mass density, $\mathbf{V}$ is the fluid velocity, $\mathbf{B}$ is the magnetic field, p is the mechanical pressure. The boundary conditions on $\mathbf{B}$ and $\mathbf{V}$ are

$$V_r(r = R) = 0\,, \qquad B_r(r = R) = 0\,, \tag{4}$$

where R is the radius of the loop transverse to the magnetic field. Using Equation (4) in the divergence of Equation (1) gives a relation between p, $\mathbf{V}$, and $\mathbf{B}$ as

$$\nabla^2 p = \frac{1}{4\pi}\nabla \cdot [(\nabla \times \mathbf{B}) \times \mathbf{B}] - \nabla \cdot \rho[(\mathbf{V}\cdot\nabla)\mathbf{V}] + \nabla \cdot (\rho \mathbf{g})\,. \tag{5}$$

Following the procedure in Montgomery *et al.* (1978) and Krishan (1982), we find that the lowest energy state of the plasma system is a force free state characterized by the following configuration of the fields:

$$\mathbf{B} = \xi(0, 0, 1)\lambda(0, 0, 1)c(0, 0, 1)\left[\hat{e}_\theta\left(-\frac{\partial \psi}{\partial r}\right) + \hat{e}_z \lambda(0, 0, 1)\psi\right], \tag{6}$$

$$\mathbf{V} = \eta(0, 0, 1)\lambda(0, 0, 1)c(0, 0, 1)\left[\hat{e}_\theta\left(-\frac{\partial \psi}{\partial r}\right) + \hat{e}_z \lambda(0, 0, 1)\psi\right], \tag{7}$$

$$p = n(z)k_B T(r), \qquad n(z) = n_0 \exp\left[-\frac{m_i g}{k_B T} z\right], \tag{8}$$

$$T(r) = \frac{m_i}{k_B} \lambda^4(0,0,1)\,|\eta^2(0,0,1)|\,c^2(0,0,1)\,[x\{J_0^2(x) + J_1^2(x)\} - J_1(x)J_0(x)] + T_0, \tag{10}$$

$$\frac{\partial T(r)}{\partial r} = \frac{m_i}{k_B} \lambda^5(0,0,1)\,|\eta^2(0,0,1)|\,c^2(0,0,1)J_1^2(x)/x, \tag{11}$$

where $T = T_0$ at $r = 0$ and (r, θ, z) are cylindrical coordinates with Z being distance along the loop, $x_0 = \lambda R$; $x = \lambda r$; $\lambda(0,0,1) \equiv \lambda = (I_z/c\psi_t)$; I_z is the current, ψ_t is the toroidal flux, c is the speed of light, $\xi(0,0,1)$ nd $\eta(0,0,1)$ are the expansion coefficients of the fields for the lowest mode ($n = 0 = m$), $c(0,0,1)$ is a normalization constant and the J's are the Bessel functions. Equation (10) describes the radial temperature structure in the lowest energy state of the plasma loop. Figure 1 shows the radial temperature profile of a loop.

3. Spatial Line Profile

Coronal loops have been observed in UV and EUV line emission of several elements in different ionization states which may be present under the right local temperature conditions. Below, we calculate the line flux for the lines C II, C III, O IV, O VI, Ne VII,

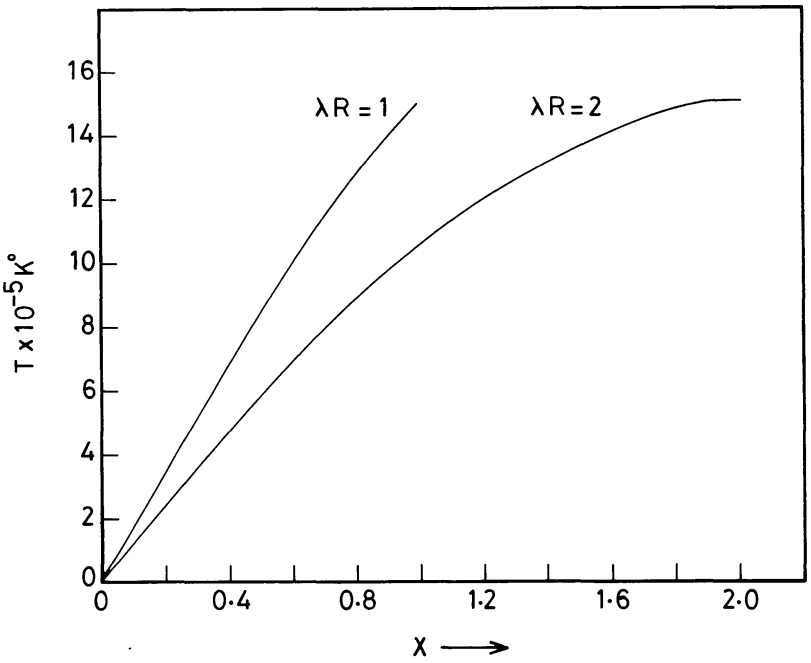

Fig. 1. Radial temperature variation in coronal loops. Curve (1) is for $\lambda R = 1$ and curve (2) is for $\lambda R = 2$.

and Mg X which have mean temperatures of formation 5×10^4 K, 9×10^4 K, 2×10^5 K, 3×10^5 K, 6×10^5 K, and 1.4×10^6 K, respectively. The line flux of an optically thin line is given as

$$F_\gamma(\text{ergs cm}^{-2}\,\text{s}^{-1}\,\text{sterad}^{-1}) = 2.2 \times 10^{-15} Af \int n_e^2 g T_e^{-1/2} \times \exp[-\Delta E/k_B T] R_i \, dz \qquad (12)$$

according to Dupree (1972), Withbroe (1975), and Levine and Withbroe (1977). Here A is the abundance of the element producing the line with respect to hydrogen, f is the oscillator strength, g is Gaunt factor, ΔE is the excitation energy and R_i is the fractional ion concentration. Since in the present model temperature T is a function of r only, one can plot $F_\gamma[2.2 \times 10^{-15} \int n_e^2 \, dz]^{-1}$ vs x in order to see the relative variation of spatial width from line to line. The numerical values of the element and line parameters have been taken from Dupree (1972), Allen and Dupree (1969), and are given in Table I.

TABLE I

Line	Formation temperature (K)	Wavelength (Å)	A	f	$(T^{-1/2} e^{-\Delta E/k_B T} R_i)_{\max}$	ergs cm^{-2} s^{-2} sterad^{-1}
C II	5×10^4	1335	$10^{8.5}$	0.101	1×10^{-4}	–
C III	9×10^4	977	$10^{8.5}$	0.432	3.6×10^{-4}	9×10^2
O IV	2×10^5	554	$10^{8.6}$	0.266	4×10^{-4}	4.7×10^1
O VI	3×10^5	1032	$10^{8.6}$	0.131	3×10^{-4}	2.16×10^2
Ne VII	6×10^5	465	$10^{7.5}$	0.393	2×10^{-4}	3.86×10^1
Mg X	1.4×10^6	625	$10^{7.5}$	0.042	1.84×10^{-4}	4.19×10^1

In order to calculate the spatial profile of temperature, we need to know the value of $\lambda^2\eta^2(0, 0, 1)$ which is a measure of the turbulent velocity in the fluid. We fixed it by requiring that $T = T_0 = 6 \times 10^3$ K at the axis of the loop at $x = 0$ and T = average formation temperature of Mg X at the surface. Using the typical values of the current density and toroidal flux in the loop (Krishan, 1982), for example, for the current density $J_z = 3 \times 10^5$ statamp cm^{-2}, the thickness of the current sheet $d = 10^5$ cm and the axial magnetic field strength $B \sim 1.5$ G, we find

$$\lambda = \frac{2\pi J_z \, dR}{c\pi R^2 B_z} \sim \frac{2}{R} ,$$

where R is the radius of the loop. We define the surface of the loop by $\lambda R = x = 2$. Demanding $T = 1.5 \times 10^6$ K at $x = 2$ requires $\lambda^2\eta^2(0, 0, 1) = 10^{14}$ (cm s^{-1})^2. From Equation (7) we find

$$V^2 = V_z^2 + V_\theta^2 = \eta^2\lambda^2 c^2 (J_0^2\lambda^2 + J_1^2\lambda^2)$$
$$= \eta^2\lambda^2 [J_0^2(x) + J_1^2(x)] \, [2J_1^2(x_0) + J_0^2(x_0) - J_0(x_0)J_2(x_0)]^{-1} . \qquad (13)$$

From the above expression, using $\eta^2\lambda^2 \sim 10^{14}$ (cm s^{-1})^2, we find a random velocity of 90 km s^{-1} near the surface of the loop at $x = 2$ and a random velocity of 70 km s^{-1} at the axis in the core, at $x = 0$. Turbulent velocities as high as $V_{\rm rms} \approx 50$ km s^{-1} have been inferred from the line widths of transition region and coronal lines Feldman and Behring (1974). Transient small scale flow velocities between 0 and 150 km s^{-1} have been suggested from the observation of the EUV emissions of O V, Si IV, and C IV from rockets and OSO-8 Foukal (1976), Athay *et al.* (1981), and Priest (1982). A velocity of 30 km s^{-1} at $x = 0$ would fix the value of $\eta^2\lambda^2$ to be $\sim 2 \times 10^{13}$ (cm s^{-1})^2 from Equation (13). Using Equation (10), we find $T = 4 \times 10^5$ K at $x = 2$. This is near the formation temperature of O VI line. Thus in order to accomodate Mg X line, one needs a higher value of R. We find for $V \approx 30$ km s^{-1}, $T \approx 30$ km s^{-1}, $T \approx 1.5 \times 10^6$ K at $\lambda R \approx 7$. Thus the picture that emerges from the above exercise is that for a given range of lines (or their formation temperatures) and for a given radius R, smaller turbulent velocities require larger value of λ which in turn requires either large current density or large thickness of the current sheath or small magnetic fields. Thus for $V \approx 30$ km s^{-1}, in order to get $\lambda R \approx 7$ one needs to increase the quantity $(J_z d/B_z)$ by a factor of 3.5. The Doppler shift of the lines is given by the V_z component of the velocity and is proportional to $J_0(x)$. Thus this model predicts smaller Doppler shift for hotter lines since $J_0(x)$ decreases as x increase. If the loop parameters are such that $x \geq 2.5$, then at $x \gtrsim 2.5$, the V_z reverses its sign and so will the Doppler shift. A plot of $F_\gamma[2.2 \times 10^{-15} \int n_e^2\, dz]^{-1}$ vs x is shown in Figures 2 and 3 for several lines indicated

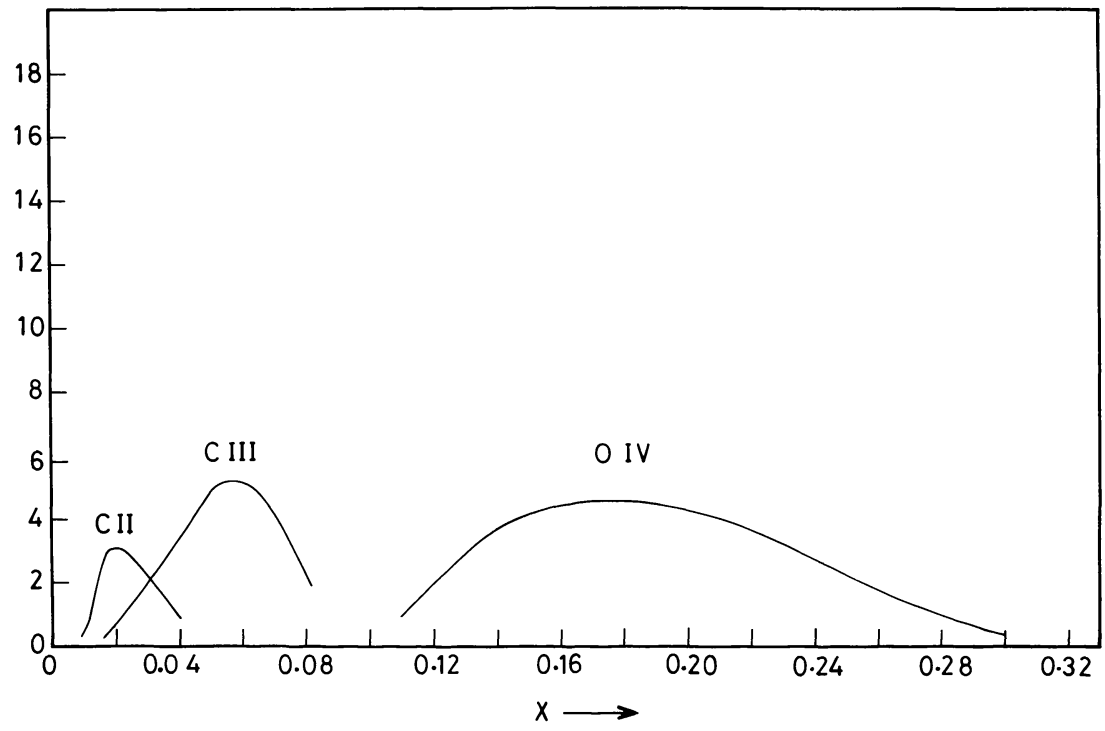

Fig. 2. Spatial profile of lines. The vertical axis represents $(F_\gamma/10^3)\,[2.2 \times 10^{-15} \int n_e^2\, dz]^{-1} \equiv$ $\equiv (F_\gamma(z)/10^3)$ for C II; $(F_\gamma(z)/10^4)$ for C III and O IV.

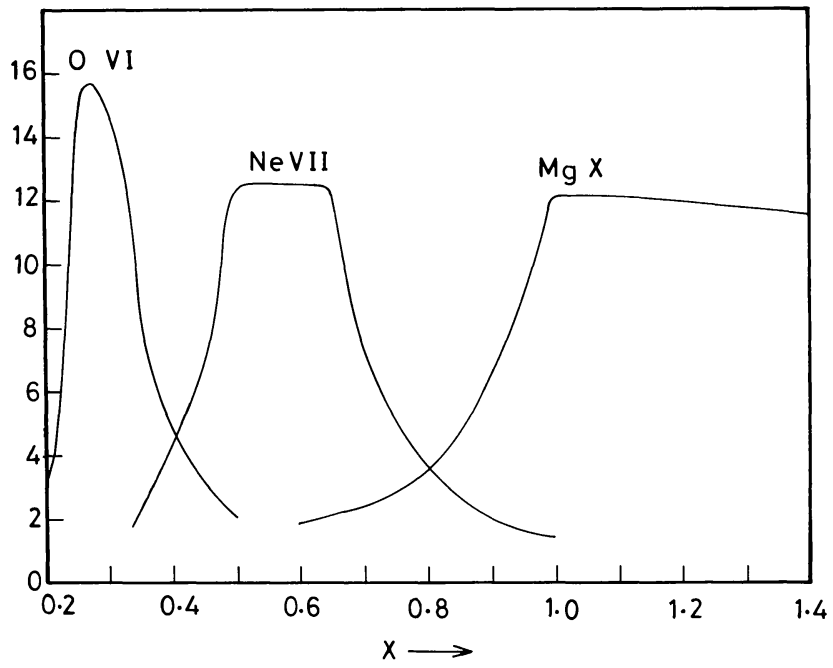

Fig. 3. Spatial profile of lines. The vertical axis represents $(F_\gamma(z)/10^3)$ for O VI; $(F_\gamma(z) \times 5/10^3)$ for Ne VII and $(F_\gamma(z) \times 5/10^2)$ for Mg X.

on the curves using $\lambda^2\eta^2 \approx 10^{14}$ (cm s^{-1})^2. The vertical flux scale is different for each line and is explained in the figure captions. The spatial profiles clearly exhibit the broader nature of hot emission lines. The width of a line increases as its average formation temperature increases. This aspect certainly agrees with the findings of Levine and Withbroe (1977).

In this statistical magnetohydrodynamic study, the lowest mode describes only the radial variation of plasma pressure. It is possible to study the three dimensional profiles of density, temperature and magnetic field by the inclusion of higher energy states. Thus, for example, superposition of (m = 0, 1, n = 0, 1) modes gives the three-dimensional configuration. Calculations of the longitudinal structure can be compared with the results of Rosner *et al.* (1978) who found the temperature maximum to be located at the apex of the loop. Since the lowest energy state has been able to account for the transverse temperature structure of the coronal loops (i.e. those with a cool core and a hot sheath) we have restricted ourselves in the present study only to this mode. Configurations resulting from the superposition of Chandrasekhar–Kendall functions will be presented in a later publication.

4. Conclusion

It is found from the statistical treatment of magnetohydrodynamic plasma that the steady state of a coronal loop can be described by a single Chadrasekhar–Kendall function corresponding to the state of minimum energy. The radial temperature profile agrees well with that of empirical cool and hot sheath models and observed spatially

broader emission of hotter lines. Three-dimensional configuration resulting from the superposition of Chadrasekhar–Kendall functions may account for other features like the temperature maximum at the apex of the loop.

References

Allen, J. W. and Dupree, A. K.: 1969, *Astrophys. J.* **155**, 27.
Athay, R. G., White, O. R., Lites, B. W., and Bruner, E. C.: 1980, *Solar Phys.* **66**, 357.
Dupree, A. K.: 1972, *Astrophys. J.* **178**, 527.
Dupree, A. K. and Reeves, E. H.: 1971, *Astrophys. J.* **165**, 599.
Foukal, P. V.: 1975, *Solar Phys.* **43**, 327.
Foukal, P. V.: 1976, *Astrophys. J.* **210**, 575.
Foukal, P. V.: 1978, *Astrophys. J.* **223**, 1046.
Foukal, P. V., Huber, M. C. E., Noyes, R. W., Reeves, E. H., Schmahl, E. J., Timothy, J. G., Vernazza, J. E., and Withbroe, G. L.: 1974, *Astrophys. J.* **193**, L143.
Hood, A. W. and Priest, E. R.: 1979, *Astron. Astrophys.* **77**, 233.
Krieger, A. S., de Feiter, L. D., and Vaiana, G. S.: 1976, *Solar Phys.* **47**, 117.
Krishan, V.: 1982, 'Radial Temperature Structure of Active Region Loops' (preprint).
Levine, R. H. and Altschuler, M. D.: 1974, *Solar Phys.* **36**, 345.
Levine, R. H. and Withbroe, G. L.: 1977, *Solar Phys.* **51**, 83.
Montgomery, D., Turner, L., and Vahala, G.: 1978, *Phys. Fluids* **21**, 757.
Poletto, G., Vaiana, G. S., Zomback, M. V., Krieger, A. S., and Timothy, A. F.: 1975, *Solar Phys.* **44**, 83.
Priest, E. R.: 1978, *Solar Phys.* **58**, 57.
Priest, E. R.: 1982, *Solar Magnetohydrodynamics*, D. Reidel Publ. Co., Dordrecht, Holland, p. 45.
Rosner, R., Tucker, W. H., and Vaiana, G. S.: 1978, *Astrophys. J.* **220**, 643.
Vaiana, G. S. and Rosner, R.: 1978, *Ann. Rev. Astron. Astrophys.* **16**, 393.
Withbroe, G. L.: 1975, *Solar Phys.* **45**, 301.